

RoadMind: Towards a Geospatial AI Expert for Disaster Response

Ahmed El Fekih Zguir, Ferda Ofli, Muhammad Imran

Qatar Computing Research Institute
azguir@hbku.edu.qa, fofli@hbku.edu.qa, mimran@hbku.edu.qa

Abstract

Large Language Models (LLMs) have shown impressive performance across a range of natural language tasks, but remain limited in their ability to reason about geospatial data, particularly road networks, distances, and directions. This gap poses challenges in disaster scenarios, where spatial understanding is critical for tasks such as evacuation planning and resource allocation. In this work, we present RoadMind, a self-supervised framework that enhances the geospatial reasoning capabilities of LLMs using structured data from OpenStreetMap (OSM). Our automated pipeline extracts road infrastructure data for a given city and converts it into multiple supervision formats tailored to key spatial tasks. We pretrain and fine-tune LLMs on these representations using QLoRA adapters and 4-bit quantized models. We evaluate our approach on three disaster-prone cities with varying global representation, Los Angeles, Christchurch, and Manila, across tasks such as road segment identification, nearest road retrieval, and distance/direction estimation. Our results show that models trained via RoadMind significantly outperform strong baselines, including state-of-the-art LLMs equipped with advanced prompt engineering. This demonstrates the potential of structured geospatial data to enhance language models with robust spatial reasoning, enabling more effective offline AI systems for disaster response.

Introduction

The frequency and severity of disasters have risen in recent years due to climate change, population growth, and political instability (European Commission, Joint Research Centre 2024; UNDRR 2020), resulting in human casualties, infrastructure damage, and socio-economic loss. To reduce these impacts, humanitarian organizations and governments rely on the disaster management cycle, which includes mitigation, preparedness, response, and recovery (University of Central Florida 2025).

Artificial Intelligence has increasingly supported each phase of this cycle. AI systems for flood prediction, wildfire detection, early warning, and damage assessment (Nearing et al. 2024; Singh, Ang, and Srivastava 2025; Kolivand et al. 2024; WFP, Google research 2024; Imran et al. 2014) have proven valuable, especially during preparedness and response.

Copyright © 2026, Association for the Advancement of Artificial Intelligence (www.aaai.org). All rights reserved.

More recently, Large Language Models (LLMs), which are trained on vast internet scale data and possess broad world knowledge, have taken the spotlight due to their impressive capabilities in contextual understanding, text generation, generalizability, zero-shot reasoning, and emergent behaviors (Kojima et al. 2022; Wei et al. 2022). These strengths have led to the adaptation of LLMs in crisis situations, including summarizing real-time crisis updates from social media (Pereira, Lotufo, and Nogueira 2023), classifying requests and offers of aid during emergencies (El Fekih Zguir, Ofli, and Imran 2025), and more.

However, LLMs struggle with geospatial reasoning and knowledge (Figure 1). They have difficulty interpreting maps, coordinates, road networks, and spatial relationships like distance and direction (Ji et al. 2025a; Cohn and Blackwell 2024; Bhandari, Anastasopoulos, and Pfoser 2023). This gap is critical, as road network understanding is essential across all disaster phases, from evacuation planning to resource routing and situational awareness.

While GIS tools can perform complex geospatial tasks, they typically require expert users and stable internet access, both of which are often lacking in disaster zones and developing regions (Rector 2022). This highlights the need for offline-capable, geospatially aware AI tools that can support responders in the field.

OpenStreetMap (OSM) (Haklay and Weber 2008), a global crowdsourced geospatial database of roads, buildings, and infrastructure, has been extensively used in past disaster responses (Klaptocz 2015; Herfort et al. 2021; Humanitarian OpenStreetMap Team 2023). Yet, LLMs are not trained to interpret structured data from OSM, leaving this rich resource largely unused.

Towards developing fully offline, geospatially-aware expert systems that can support all phases of the disaster management cycle, we leverage the abundant structured data available in OSM to pretrain and fine-tune off-the-shelf foundation models. In this study, we make the following contributions:

1. We demonstrate the limitations of state-of-the-art open-source LLMs in handling core geospatial tasks such as interpreting coordinates, estimating distances, inferring directions, and reasoning about road networks.
2. We propose geospatial data representations, derived from OSM, specifically designed to train LLMs to reason

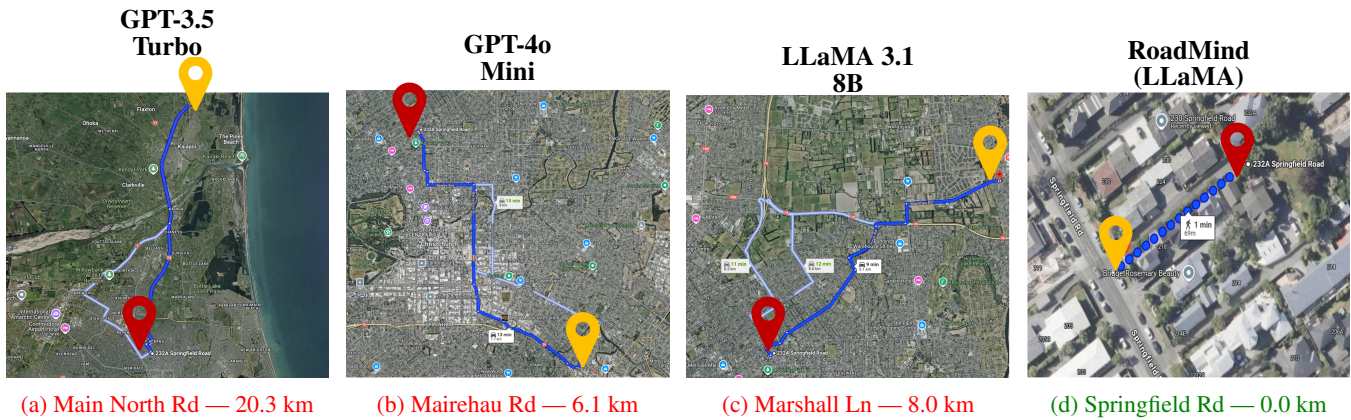


Figure 1: Responses to the query: *Which road is closest to the geo-coordinates (-43.5103, 172.6318)?* Only RoadMind (d) correctly identifies *Springfield Road*. Other models return incorrect roads several kilometers away.

about road infrastructure and spatial relationships.

3. We develop a fully automated framework that transforms raw OSM data into these representations and uses them to pretrain and fine-tune “road expert” LLMs for specific cities.
4. We evaluate our approach on three disaster-prone cities (figure 3): Christchurch (New Zealand), Los Angeles (United States), and Manila (Philippines). These locations were chosen as they vary in size, global familiarity, and language use, allowing us to assess the adaptability and robustness of our system across diverse settings.

Related Work

Several recent studies have investigated the geospatial capabilities of LLMs and explored ways to enhance their spatial reasoning. Foundational work by Bhandari, Anastasopoulos, and Pfoser (2023) demonstrated that while modern LLMs possess some latent geographic knowledge, they struggle with basic spatial reasoning tasks such as interpreting coordinates, understanding spatial prepositions, and identifying relative positions of cities. Further evaluation by Ji et al. (2025b) confirmed that even top-performing models like GPT-4 exhibit limited accuracy in identifying topological spatial relations between geometries. Roberts et al. (2023) similarly assessed GPT-4’s capabilities across a range of geographic tasks, such as estimating distances, reasoning over travel routes, and outlining countries, revealing a mix of promising behaviors and clear limitations. These results are consistent with findings by Gurnee and Tegmark (2024), who show that models like LLaMA-2 do learn spatial representations internally, but these are not sufficiently surfaced for robust geospatial reasoning.

To improve such capabilities, several works have proposed augmenting LLMs with structured geospatial data, particularly OSM. Manvi et al. (2024) introduce GeoLLM, a prompting-based framework that supplements LLMs with auxiliary OSM context such as nearby place names or amenities when querying coordinates. This augmentation significantly improved performance on tasks like population and economic prediction. Our work extends this idea

by directly encoding OSM knowledge into the model via pretraining and fine-tuning, rather than relying on test-time augmentation. Unlu (2023) also fine-tune a small LLM using artificial OSM-derived question-answer pairs to provide a linguistic interface to urban geospatial data. While their work is limited to shallow summaries and lacks task benchmarks, it demonstrates the promise of fine-tuning models on OSM-derived inputs. Li et al. (2022, 2023) propose contrastive and coordinate-aware pretraining methods that align geospatial and linguistic contexts, improving performance on geo-entity linking, typing, and relation extraction. These efforts highlight the potential of structured data to bridge the gap between language and geography.

Domain-specific models have also emerged to support geospatial and urban tasks. Deng et al. (2024) present K2, a foundation model for geoscience trained on domain-specific corpora, while Huang et al. (2022) develop ERNIE-GeoL by integrating geographic graphs into pretraining for real-world map applications. In the urban context, Feng et al. (2025) introduce CityGPT, which combines instruction tuning with urban datasets to improve LLMs’ ability to handle city-specific reasoning tasks. Similarly, Balsebre, Huang, and Cong (2024) fine-tune a model, LAMP, on point-of-interest (POI) data to enable local recommendations with reduced hallucination. While promising, these works focus on POIs and urban knowledge at a coarse level. In contrast, our approach encodes detailed road network structure and supports fine-grained geospatial reasoning, which is critical in time-sensitive disaster scenarios.

Other lines of research focus on tool-augmented LLMs. Zhang et al. (2024) propose GeoGPT, which enables non-experts to solve spatial problems by allowing the model to plan and execute GIS operations such as buffering or intersection. Jiang et al. (2024) introduce a multi-agent system where a controller LLM decomposes queries and delegates subtasks to domain-specific AI modules. These tool-augmented approaches are powerful but assume access to robust infrastructure, an assumption that does not always hold in disaster-affected regions. Our work instead focuses on building standalone models that can reason about roads, dis-

tances, and directions without external calls, making them more suitable for offline and resource-constrained deployments.

Lastly, while models like CityFM (Balsebre et al. 2024) and SARN (Chang et al. 2023) demonstrate strong performance on urban and road-level tasks, they do not make use of off-the-shelf LLMs nor do they target language-based geospatial reasoning. Our work fills this gap by adapting LLMs specifically for road-based spatial reasoning using high-fidelity OSM-derived inputs, showing strong gains across core disaster-relevant tasks such as distance estimation, direction inference, segment identification, and nearest road prediction.

OpenStreetMap Preliminaries

OpenStreetMap (OSM) is a collaborative geospatial database whose road network is built upon two fundamental primitives:

- **Nodes:** Geographic points defined by a latitude and longitude.
- **Ways:** Ordered sequences of nodes that define linear features like roads..

Both nodes and ways can carry descriptive *tags*—key-value pairs encoding attributes, such as `highway=primary` or `maxspeed=80`.

We define a road segment as a contiguous portion of a road with consistent attributes (e.g., speed limit, lane count, road type). Segments are derived from OSM ways by merging contiguous paths that share the same tags and are connected in the road graph, which we construct using the `osmnx` library.

For each segment s , we extract the following attributes:

- **Geometry:** An ordered list of (latitude, longitude) tuples representing the path of the segment.
- **Road Name:** From the `name` tag ("Ilam Road").
- **Road Type:** From the `highway` tag (e.g., `primary`).
- **Speed Limit:** From the `maxspeed` tag.
- **Lane Count:** From the `lanes` tag.
- **Segment Length:** Computed in meters using the Haversine formula via the `osmnx` library.

All coordinates follow the WGS84 (EPSG:4326) system, consistent with OSM and popular tools like Google Maps.

Methodology

We introduce **RoadMind** (figure 2), a modular training framework that transforms structured geographic data into supervision signals for LLMs. Given a city name, our fully automated pipeline extracts OSM data and converts it into LLM-centric geospatial representations. We further augment this with additional data formats that are not OSM-specific but still encode spatial relationships (e.g., relative directions and distance pairs). These various representations are then standardized into text-to-text formats suitable for both continual pretraining and instruction fine-tuning.

Our training procedure follows a two-stage approach. We first perform geospatial pretraining to embed spatial knowledge into the model’s parameters using QLoRA adapters and 4-bit quantized base models. We then fine-tune the same adapters on downstream geospatial tasks, such as question answering over road networks. All experiments are conducted using three base LLMs across three cities selected for their varying levels of representation in common training corpora: Los Angeles (a globally well-represented urban center), Christchurch (a medium-size city with modest coverage), and Manila (a large but underrepresented city in many web-scale datasets).

To benchmark performance, we evaluate our models against state-of-the-art, publicly available LLMs enhanced through strong prompt engineering strategies, including chain-of-thought (CoT), few-shot examples, contextual grounding, and query-specific few shot learning (QSF) (El Fekih Zguir, Ofli, and Imran 2025). These strategies serve as informed baselines or “cheat sheets,” allowing us to isolate the benefit of model-internal geospatial knowledge from externally provided guidance.

Geospatial Representations

To enable LLMs to reason effectively about road infrastructure, we introduce a set of geospatial representations that convert structured OpenStreetMap (OSM) data into natural language formats. These representations transform spatial inputs, such as road names, segment geometries, and coordinates, into text-to-text supervision signals, enabling models to perform tasks similar to spatial lookup, aggregation, and inference.

We divide our representations into two categories: (1) **Core Representations**, which encode fundamental road network structure from OSM, and (2) **Spatial Reasoning Representations**, which support orientation, measurement, and connectivity beyond OSM’s explicit schema. Together, they form a curriculum for embedding geospatial knowledge into language models.

Notation Let $\mathbf{p} = (lat, lon) \in R^2$ denote a geographic point in the WGS84 coordinate system. A road segment s is defined by a polyline geometry $\mathbf{g} = [\mathbf{p}_1, \dots, \mathbf{p}_m]$. A named road R consists of a set of segments $\{s_1, \dots, s_n\}$ sharing the same name tag. Each segment has metadata $meta(s)$, including road type, speed limit, lane count, and length. The metadata of a full road is:

$$meta(R) = \text{aggregate}(meta(s_1), \dots, meta(s_n))$$

Core Representations Our core supervision formats, **Point-to-Segment (P2S)**, **Segment-to-Info (S2I)**, and **Road-to-Info (R2I)**, are designed to teach foundational spatial reasoning grounded in road network geometry and semantics.

Road-to-Info (R2I): Models learn to associate a road name R with its aggregated physical and regulatory metadata, $meta(R)$, encouraging abstraction from text labels to network structure. The input is a road name R , and the output is its corresponding metadata.

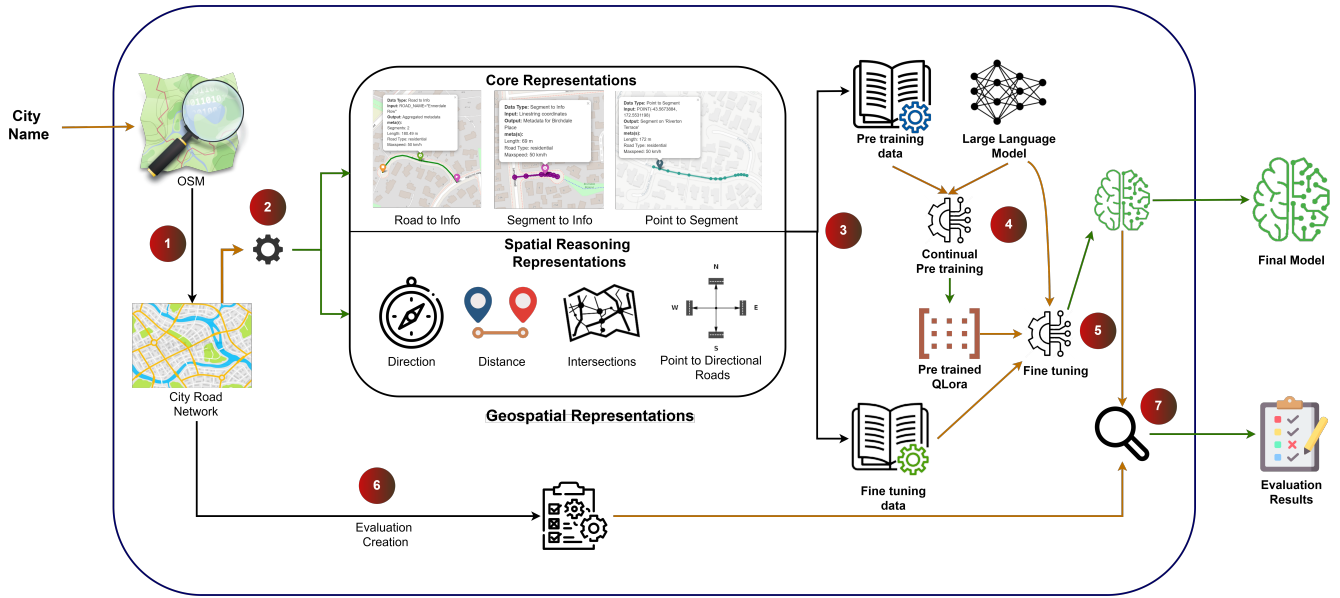


Figure 2: Overview of the proposed ROADMIND framework. Brown arrows are inputs and green arrows are outputs.

Point-to-Segment (P2S): This format builds spatial grounding by training the model to localize a geographic coordinate \mathbf{p} and retrieve the road segment s it lies on, along with $\text{meta}(s)$. The input is a geographic point \mathbf{p} , and the output is the segment geometry \mathbf{g} and associated metadata.

Segment-to-Info (S2I): Enables the model to infer semantic properties of a road segment from its raw geometry. Given a segment geometry \mathbf{g} as input, the model predicts the corresponding metadata $\text{meta}(s)$.

Together, these core formats form the foundation for teaching models to interpret and reason about structured road infrastructure.

Spatial Reasoning Representations We extend the model’s capabilities with formats that support directional, metric, and topological reasoning.

Road-to-Connected-Roads: Supports topological reasoning by identifying roads that intersect a given road and the coordinates of their intersection points. The input is a road name R , and the output is a list of connected roads with their intersection coordinates.

Point-Pair-to-Distance: Trains the model to estimate haversine distance between two coordinates. Given points \mathbf{p}_1 and \mathbf{p}_2 as input, the output is the distance in meters.

Point-Pair-to-Direction: Encourages the model to infer compass direction from a pair of coordinates. The input is two points \mathbf{p}_1 and \mathbf{p}_2 , and the output is the corresponding cardinal direction.

Point-to-Directional-Roads: Enhances spatial exploration and directional awareness by retrieving the nearest road in each of the eight cardinal directions from a reference point. The input is a point \mathbf{p} , and the output is a mapping from direction to the nearest road name and distance.

We generate training points for the point-to-directional roads representation using a density-aware spatial sampling strategy. The AOI is divided into a uniform grid, and the number of points sampled in each cell is proportional to the local density of road segments. This ensures that training data is concentrated in more populated areas of the road network, allowing the model to better learn spatial relationships in regions where detailed reasoning is most needed. For each of these sampled points, we get the nearest road in each direction, as shown in Alg. 1.

These supervision formats collectively teach LLMs to localize points, measure distances, and reason about connectivity and direction using natural language and raw coordinates. Together, they provide a foundation for geospatial reasoning in downstream tasks.

Training Setup

RoadMind follows a two-stage training approach: **continual pretraining** followed by **instruction fine-tuning**. Continual pretraining allows the model to internalize new domain knowledge, in this case, road network structure and spatial relationships, without forgetting prior capabilities, as shown in (Gururangan et al. 2020). We then fine-tune the model using instruction-style prompts to align it with downstream geospatial tasks, following a setup similar to (Deng et al. 2024).

For efficiency in both memory and computation, we adopt QLoRA (Dettmers et al. 2023), using 4-bit quantized base models and lightweight LoRA adapters. The same adapters trained during pretraining are reused during fine-tuning, preserving the embedded geospatial knowledge.

Each data representation described in Section is converted into two formats: (1) a pretraining version, structured like a compact Wikipedia-style document with a brief title

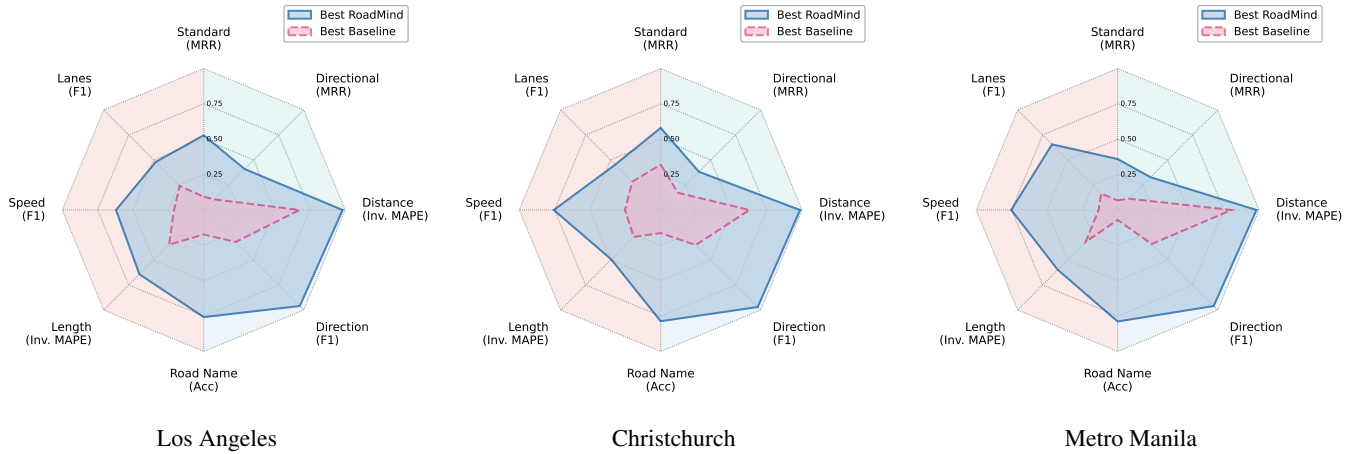


Figure 3: Radar plots comparing best RoadMind and baseline models across task categories: metadata prediction, spatial calculation, and road retrieval. All metrics are increasing (inverse MAPE used).

Algorithm 1: Directional Nearest Road Retrieval

Input: Reference point \mathbf{p} , road network G , radius r

Output: Dictionary D : direction \rightarrow (road name, distance)

```

1: Initialize  $D \leftarrow \{\}$ 
2: for each direction  $d \in \{N, NE, E, SE, S, SW, W, NW\}$ 
   do
3:   Define angular sector  $S_d$  centered at  $\mathbf{p}$  with radius  $r$ 
4:   Clip road network to sector:  $G_d = G \cap S_d$ 
5:   Set  $min\_dist \leftarrow \infty$ ,  $closest \leftarrow None$ 
6:   for each named segment  $s \in G_d$  do
7:     Project  $\mathbf{p}$  onto  $s$  to get projected point  $\mathbf{p}'$ 
8:     Compute distance  $d = dist(\mathbf{p}, \mathbf{p}')$ 
9:     if  $d < min\_dist$  then
10:       $min\_dist \leftarrow d$ 
11:       $closest \leftarrow (\text{name of } s, d)$ 
12:     end if
13:   end for
14:   if  $closest \neq None$  then
15:      $D[d] \leftarrow closest$ 
16:   end if
17: end for
18: return  $D$ 

```

and factual content, and (2) an instruction fine-tuning version, which includes at least five diverse prompt formulations for each input-output pair.

We train three open-weight LLMs, LLaMA 3.1 8B, Mistral 7B v0.3, and Qwen 3 8B, on each city independently. Additionally, we train a multi-city version of Mistral using data from all cities combined to evaluate generalization across geographies.

Evaluation Tasks

We evaluate the model’s geospatial reasoning across three task categories: road metadata prediction, spatial calculation, and road retrieval.

Road Metadata Prediction For a given point on a randomly selected road segment, the model predicts the segment’s attributes: maxspeed, number of lanes, segment length, and road name. To prevent simple memorization, the point is interpolated along the segment’s geometry rather than being an existing OSM node.

Metrics: Road name is evaluated using accuracy; segment length via Mean Absolute Percentage Error (MAPE) and the percentage of predictions within $\pm 30\%$; and maxspeed and lane count using accuracy and macro F1.

Spatial Calculation These tasks involve reasoning about a pair of random points (p_1, p_2) within the city.

Distance Estimation: Predict the haversine distance between p_1 and p_2 (in meters), evaluated using MAPE.

Direction Estimation: Predict the cardinal direction from p_1 to p_2 , categorized into eight directions (N, NE, E, . . .). Evaluated using macro Precision, Recall, and F1.

Road Retrieval Given a query point p , the model predicts nearby roads.

Standard Retrieval: Predict the nearest road to p .

Directional Retrieval: Predict the name of the closest road in each of the 8 cardinal directions from p .

Metrics: Metrics compare the single predicted road \hat{r}_i against a ground-truth list of roads G_i sorted by distance from the query point

- **Hit@k:** Fraction of predictions where the predicted road \hat{r}_i is among the top- k ground-truth nearest roads¹:

$$\text{Hit}@k = \frac{1}{n} \sum_{i=1}^n 1 \left\{ \hat{r}_i \in G_i^{(k)} \right\}$$

- **MRR:** Mean Reciprocal Rank of the predicted road in the sorted ground-truth list.
- **Directional Hit@k:** The Hit@k metric applied to the Directional Road Retrieval task, averaged across all eight directions.

¹Note that this definition differs from the standard Hit@k.

- **Accuracy@1km:** Fraction of predictions where the predicted road lies within 1 km of the query point

Baselines and Prompting Enhancements

To evaluate ROADMIND, we compare against strong open-source instruction-tuned models: Qwen 3 8B, LLaMA 3.1 8B, and Mistral 7B v0.3, as well as GPT-4o Mini, which is used only with prompting due to cost constraints.

We use two prompting settings for the open-source models: **direct prompting** (simple, task-specific queries without enhancements) and **cheat-sheet prompting**, which combines several advanced strategies: **Chain-of-Thought (CoT)** reasoning, **few-shot learning**, **contextual grounding** (injecting structured OSM information, as in (Manvi et al. 2024)), and **Query-Specific Few-shot (QSF)** learning (El Fekih Zguir, Ofli, and Imran 2025), which retrieves semantically similar few-shot examples.

QSF is applied only to road retrieval tasks. Following (El Fekih Zguir, Ofli, and Imran 2025), we build a database of 1,000 sampled points in the area of interest (AOI), each annotated with nearest and directional roads. For a new test point p , we retrieve its 10 closest examples using haversine distance and use them as few-shot demonstrations, leveraging spatial locality.

Contextual grounding is applied to all tasks except spatial reasoning. For road retrieval, the prompt includes road names within a 4km radius of the query point. For metadata prediction, we provide distributional hints such as typical `maxspeed` values, lane counts, segment lengths, and nearby road names. For distance and direction estimation, neither contextual grounding nor QSF is applicable; only Chain-of-Thought and few-shot prompting are used.

Evaluation and Results

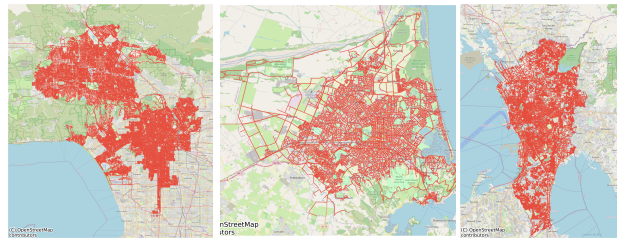
Cities Overview

We evaluate our models on three disaster-prone cities, Christchurch, Los Angeles, and Metro Manila, chosen for their diversity in size, infrastructure, and language (Figure 4). Metro Manila’s predominant use of Tagalog enables us to examine the impact of linguistic bias in LLMs, while the variation in road network scale allows us to assess generalization across urban densities.

Table 2 summarizes key statistics. Los Angeles spans the largest area (1990.7 km²) and has the longest road network (20,847 km). Metro Manila, though smaller in area (973.8 km²), contains the densest network with over 149,000 segments. Christchurch is the smallest and sparsest, with just 26,186 segments over 900.5 km².

Results

Table 1 presents results across three cities, 18 metrics, and four model groups, with performance color-coded (darker is better). We structure the analysis around three guiding questions: (i) *How far can prompting alone go?* (ii) *What does ROADMIND add?* (iii) *How do city characteristics affect performance?*



Los Angeles Christchurch Metro Manila

Figure 4: Road networks of the three evaluation cities.

(i) **Prompting alone is not enough.** Instruction-tuned models with direct prompting (first three rows per city) perform poorly across all tasks. In *road retrieval*, Hit@1 never exceeds 0.004, and MRR remains below 0.01. Spatial calculation is similarly weak: distance MAPE reaches 0.56 in Los Angeles and 0.30 in Manila, while directional macro-F1 stays below 0.14. Only Christchurch shows modest success in *lanes prediction* (accuracy 0.874), which we attribute to a data artifact where most road segments have 2 lanes. Without grounding or enhancements, models often repeat high-frequency names like *Halswell Road* or fail to respond meaningfully.

(ii) **Cheat-sheet prompting improves results, but ROADMIND brings a step-change.** Advanced prompting techniques (Chain-of-Thought, Few-shot, Contextual Grounding, and QSF) boost performance: In road retrieval, metrics increase by one to two orders of magnitude (e.g., Qwen’s Hit@1 in Christchurch rises from 0 to 0.233). In metadata prediction, LLaMA’s segment length MAPE in Christchurch drops from 2.78 to 0.73. Spatial reasoning shows modest gains, but MAPE remains above 0.32 and directional F1 rarely exceeds 0.20.

ROADMIND models (bottom rows) go significantly further across all tasks. In road retrieval, they achieve top-1 accuracy@1km of 0.964 in Christchurch, 0.957 in Los Angeles, and 0.900 in Manila, representing gains of 150-430% over cheat-sheet baselines. For directional retrieval, Hit@1 reaches 0.325 in Christchurch and 0.314 in L.A., whereas no baseline exceeds 0.149. In spatial calculation, ROADMIND reduces distance MAPE to below 0.032 in all cities, and achieves directional macro-F1 of up to 0.95, demonstrating a strong grasp of spatial and angular relationships. Finally, in metadata prediction, road-name accuracy in Los Angeles triples (from 0.173 to 0.757), and lane count F1 in Manila rises by 299% (from 0.164 to 0.656).

(iii) **City-level insights.** **Christchurch** (small, homogeneous): cheat-sheet baselines already perform decently, yet ROADMIND still achieves 80–143% gains in directional retrieval. Qwen scores poorly as it often over-predicts major roads like *Halswell Road*, suggesting overfitting.

Los Angeles (large, English-speaking): the largest performance gap appears here. Despite strong coverage in pre-training data, scale and language alone are insufficient for grounded spatial reasoning.

City	Model	Road Retrieval								Spatial Calculation			Metadata Prediction							
		Standard				Directional				Dist			Road		Length		Speed		Lanes	
		H@1	H@5	A@1km	MRR	H@1	H@5	A@1km	MRR	MAPE ↓	Acc ↑	F1 ↑	Acc ↑	MAPE ↓	A@30% ↑	Acc ↑	F1 ↑	Acc ↑	F1 ↑	
Christchurch	LLaMA	0	0.003	0.013	0.002	0	0	0	0	0.695	0.22	0.14	0.002	2.7821	0.114	0	0	0	0.874	0.2332
	Mistral	0.002	0.005	0.017	0.001	0.027	0.027	0.027	0.018	1.33	0.12	0.03	0	8.3	0.016	0	0	0	0.863	0.1858
	Qwen	0	0.001	0.004	0.001	0.002	0.002	0.002	0.002	0.678	0.12	0.03	0.001	1.6582	0.235	0	0	0	0.821	0.2334
	LLaMA + cheat	0.16	0.286	0.44	0.218	0.134	0.206	0.237	0.165	0.4429	0.26	0.19	0.064	0.9429	0.289	0.655	0.1772	0.839	0.1864	0.839
	Mistral + cheat	0.169	0.347	0.595	0.252	0.092	0.112	0.124	0.101	0.6697	0.13	0.06	0.025	1.0249	0.2683	0.643	0.1869	0.821	0.2829	0.821
	Qwen + cheat	0.23	0.425	0.676	0.321	0.129	0.229	0.265	0.172	0.37248	0.45	0.31	0.163	0.7309	0.3023	0.754	0.2528	0.851	0.2367	0.851
	4o Mini + cheat	0.103	0.176	0.289	0.138	0.103	0.147	0.164	0.122	0.4409	0.45	0.35	0.039	1.1068	0.286	0.623	0.1389	0.859	0.2644	0.859
	RoadMind (LLaMA)	0.285	0.532	0.767	0.398	0.181	0.265	0.288	0.216	0.0665	0.91	0.9	0.488	0.7366	0.179	0.75	0.2939	0.718	0.1879	0.718
	RoadMind (Mistral)	0.428	0.775	0.964	0.580	0.276	0.438	0.461	0.344	0.0206	0.95	0.95	0.694	0.6175	0.410	0.812	0.4269	0.713	0.3651	0.713
	RoadMind (Qwen)	0.046	0.067	0.109	0.057	0.044	0.060	0.062	0.049	0.045	0.97	0.97	0.028	0.7557	0.160	0.461	0.1022	0.788	0.1914	0.788
RoadMind (Mistral, All)	0.401	0.731	0.918	0.538	0.325	0.458	0.472	0.382	0.015	0.78	0.77	0.786	0.506	0.529	0.9	0.7553	0.8	0.4536	0.8	
Best RoadMind	0.428	0.775	0.964	0.580	0.325	0.458	0.472	0.382	0.015	0.97	0.97	0.786	0.506	0.529	0.9	0.7553	0.8	0.4536	0.8	
vs Best Baseline (%)	+86.09	+82.35	+42.60	+80.69	+142.54	+100.00	+78.11	+122.09	-95.97	+115.56	+177.14	+382.21	-30.77	+74.99	+19.36	+198.77	-8.47	+60.34	+60.34	
Los Angeles	LLaMA	0	0.006	0.026	0.004	0.023	0.023	0.023	0.023	0.56	0.15	0.07	0	1.132	0.238	0	0	0	0.439	0.1043
	Mistral	0	0	0	0	0	0	0	0	1.38	0.23	0.08	0	6.1366	0.0245	0	0	0	0.181	0.0595
	Qwen	0	0	0	0	0.004	0.007	0.011	0.006	0.5938	0.26	0.11	0	4.8241	0.042	0.002	0.008	0.192	0.0516	0.192
	LLaMA + cheat	0.022	0.071	0.281	0.053	0.071	0.149	0.213	0.106	0.5357	0.17	0.08	0.124	0.6615	0.3358	0.469	0.1852	0.351	0.1774	0.351
	Mistral + cheat	0.023	0.074	0.272	0.053	0.028	0.049	0.072	0.038	8.175	0.1	0.06	0.046	0.6529	0.363	0.426	0.189	0.43	0.149	0.43
	Qwen + cheat	0.048	0.133	0.383	0.094	0.04	0.11	0.172	0.072	0.3233	0.46	0.32	0.175	0.906	0.3039	0.491	0.2099	0.458	0.2404	0.458
	4o Mini + cheat	0.025	0.075	0.273	0.055	0.023	0.062	0.106	0.041	0.3799	0.37	0.3	0.073	0.7182	0.324	0.296	0.1011	0.3	0.1106	0.3
	RoadMind (LLaMA)	0.342	0.758	0.956	0.519	0.269	0.497	0.537	0.364	0.116	0.85	0.83	0.643	0.5376	0.397	0.59	0.355	0.473	0.2686	0.473
	RoadMind (Mistral)	0.349	0.771	0.957	0.528	0.295	0.511	0.539	0.387	0.0183	0.93	0.93	0.702	0.3574	0.574	0.569	0.397	0.493	0.3855	0.493
	RoadMind (Qwen)	0.315	0.725	0.946	0.491	0.184	0.352	0.393	0.254	0.2791	0.96	0.96	0.600	0.4769	0.375	0.53	0.4287	0.419	0.3038	0.419
RoadMind (Mistral, All)	0.288	0.841	0.945	0.455	0.314	0.538	0.567	0.409	0.0282	0.95	0.95	0.757	0.388	0.597	0.787	0.62	0.642	0.4797	0.642	
Best RoadMind	0.349	0.841	0.957	0.528	0.314	0.538	0.567	0.409	0.0183	0.96	0.96	0.757	0.3574	0.597	0.787	0.62	0.642	0.4797	0.642	
vs Best Baseline (%)	+627.08	+532.33	+149.87	+461.70	+342.25	+261.07	+166.20	+285.85	-94.34	+108.70	+200.00	+337.57	-45.26	+64.46	+60.29	+195.38	+0.17	+99.54	+99.54	
Manila	LLaMA	0.004	0.013	0.077	0.010	0.001	0.004	0.011	0.003	0.52	0.2	0.1	0	3.4088	0.058	0	0	0	0.002	0.0005
	Mistral	0	0	0.013	0	0.001	0.003	0.007	0.002	0.3	0.09	0.02	0	7.7808	0.01	0	0	0	0.002	0.0005
	Qwen	0	0.011	0.011	0.001	0.001	0.003	0.008	0.002	0.503	0.11	0.04	0.01	3.3385	0.062	0	0	0.152	0.0388	0.152
	LLaMA + cheat	0.015	0.031	0.183	0.026	0.083	0.148	0.216	0.113	0.0701	0.16	0.09	0.029	0.7205	0.096	0.365	0.0814	0.52	0.1645	0.52
	Mistral + cheat	0.023	0.062	0.377	0.049	0.031	0.042	0.062	0.037	22.2	0.18	0.08	0.017	0.6809	0.2375	0.422	0.1014	0.633	0.1486	0.633
	Qwen + cheat	0.036	0.089	0.378	0.068	0.034	0.086	0.149	0.059	0.2476	0.39	0.3	0.07	0.798	0.2335	0.46	0.1348	0.667	0.1556	0.667
	4o Mini + cheat	0.009	0.018	0.141	0.016	0.009	0.019	0.037	0.014	0.1944	0.42	0.34	0.016	0.7158	0.339	0.355	0.0745	0.506	0.1379	0.506
	RoadMind (LLaMA)	0.146	0.345	0.763	0.242	0.211	0.381	0.432	0.283	0.0318	0.9	0.9	0.519	0.6405	0.273	0.575	0.4243	0.667	0.4709	0.667
	RoadMind (Mistral)	0.183	0.444	0.852	0.304	0.25	0.43	0.477	0.327	0.1177	0.95	0.95	0.77	0.4019	0.54	0.708	0.7201	0.742	0.6559	0.742
	RoadMind (Qwen)	0.108	0.298	0.774	0.204	0.128	0.275	0.361	0.191	0.0186	0.97	0.96	0.465	0.6902	0.181	0.556	0.5176	0.652	0.3765	0.652
RoadMind (Mistral, All)	0.241	0.531	0.9	0.36	0.256	0.423	0.469	0.328	0.026	0.97	0.96	0.788	0.4772	0.479	0.82	0.752	0.807	0.5379	0.807	
Best RoadMind	0.241	0.531	0.9	0.36	0.256	0.423	0.469	0.328	0.0186	0.97	0.96	0.788	0.4019	0.54	0.82	0.752	0.807	0.6559	0.807	
vs Best Baseline (%)	+569.44	+496.63	+138.10	+429.41	+208.43	+190.54	+120.83	+190.27	-90.43	+130.95	+182.35	+1025.71	-40.98	+59.29	+78.26	+457.86	+20.99	+298.72	+298.72	

Table 1: A detailed performance evaluation of all models across the full range of tasks and cities. For each city, the final two rows summarize the results of the best-performing RoadMind model and compare it to the strongest baseline model. Cells are color-coded by task category, with darker shades indicating superior performance on the specific metric.

City	Area (km ²)	#Segs	#Named Roads	Length (km)
Los Angeles	1990.7	135,912	8,963	20,847.4
Christchurch	900.5	26,186	4,161	4,032.0
Metro Manila	973.8	149,163	11,849	13,761.3

Table 2: Basic statistics for the three evaluation cities.

Metro Manila (dense, non-English): baseline performance is lowest, but ROADMIND achieves the largest relative gains (e.g., +569% Hit@1), demonstrating transferability across scripts and contexts.

Model-family comparison. Across all cities, **Mistral-based ROADMIND** consistently performs best, winning 15–17 out of 18 metrics. Despite being smaller (7B vs. 8B), Mistral outperforms LLaMA and Qwen, suggesting that architecture, tokenizer coverage, and pretraining data quality outweigh minor size differences. Moreover, the *multi-city variant*, trained jointly on all three cities, often outperforms single-city models. For example, it achieves a directional Hit@5 of 0.538 in L.A. vs. 0.511 with the L.A.-only model. This supports the idea that spatial knowledge generalizes across regions.

Even with strong prompting (cheat sheets), off-the-shelf LLMs underperform on geospatial tasks. ROADMIND closes this gap through continual pretraining on diverse geospatial representations that teach both core and advanced spatial

reasoning. The foundational formats (P2S, S2I, R2I) enable localization and semantic inference, while spatial formats support distance estimation, directional lookup, and road connectivity. These structured inputs instill spatial inductive biases that prompting alone cannot induce. Crucially, the benefits generalize across model families, cities, and languages, establishing ROADMIND as a robust, extensible framework for geospatially grounded language models.

Conclusion

In this work, we presented ROADMIND, a framework for augmenting large language models with geospatial reasoning capabilities through structured training on OSM-derived representations. By transforming raw road network data into diverse natural language supervision formats, we trained models to perform core spatial tasks such as localization, distance estimation, direction inference, and road retrieval. Our results show that even strong prompting strategies (*cheat sheets*)—including few-shot learning, CoT, QSF, and contextual grounding—are insufficient to induce reliable spatial understanding in LLMs. In contrast, models trained with ROADMIND achieve substantial and consistent improvements across tasks, cities, and model families, reaching state-of-the-art performance on road-based geospatial benchmarks. These gains highlight the importance of embedding spatial inductive biases through structured data. Looking ahead, ROADMIND offers a path toward offline,

general-purpose geospatial AI experts for disaster response.

References

- Balsebre, P.; Huang, W.; and Cong, G. 2024. LAMP: A Language Model on the Map. arXiv:2403.09059.
- Balsebre, P.; Huang, W.; Cong, G.; and Li, Y. 2024. City Foundation Models for Learning General Purpose Representations from OpenStreetMap. In *Proceedings of the 33rd ACM International Conference on Information and Knowledge Management, CIKM '24*, 87–97. New York, NY, USA: Association for Computing Machinery. ISBN 9798400704369.
- Bhandari, P.; Anastasopoulos, A.; and Pfoser, D. 2023. Are Large Language Models Geospatially Knowledgeable? In *Proceedings of the 31st ACM International Conference on Advances in Geographic Information Systems (SIGSPATIAL '23)*. New York, NY, USA: ACM.
- Chang, Y.; Tanin, E.; Cao, X.; and Qi, J. 2023. Spatial Structure-Aware Road Network Embedding via Graph Contrastive Learning. In *EDBT*, 144–156.
- Cohn, A. G.; and Blackwell, R. E. 2024. Evaluating the Ability of Large Language Models to Reason About Cardinal Directions. In Adams, B.; Griffin, A. L.; Scheider, S.; and McKenzie, G., eds., *16th International Conference on Spatial Information Theory (COSIT 2024)*, volume 315 of *Leibniz International Proceedings in Informatics (LIPIcs)*, 28:1–28:9. Dagstuhl, Germany: Schloss Dagstuhl – Leibniz-Zentrum für Informatik. ISBN 978-3-95977-330-0.
- Deng, C.; Zhang, T.; He, Z.; Chen, Q.; Shi, Y.; Xu, Y.; Fu, L.; Zhang, W.; Wang, X.; Zhou, C.; Lin, Z.; and He, J. 2024. K2: A Foundation Language Model for Geoscience Knowledge Understanding and Utilization. In *Proceedings of the 17th ACM International Conference on Web Search and Data Mining, WSDM '24*, 161–170. New York, NY, USA: Association for Computing Machinery. ISBN 9798400703713.
- Dettmers, T.; Pagnoni, A.; Holtzman, A.; and Zettlemoyer, L. 2023. QLORA: efficient finetuning of quantized LLMs. In *Proceedings of the 37th International Conference on Neural Information Processing Systems, NIPS '23*. Red Hook, NY, USA: Curran Associates Inc.
- El Fekih Zguir, A.; Offi, F.; and Imran, M. 2025. Detecting Actionable Requests and Offers on Social Media During Crises Using LLMs. *Proceedings of the International IS-CRAM Conference*.
- European Commission, Joint Research Centre. 2024. Humanitarian crises and disasters: the world has become a riskier place over the past decade. https://joint-research-centre.ec.europa.eu/jrc-news-and-updates/humanitarian-crises-and-disasters-world-has-become-riskier-place-over-past-decade-2024-03-18_en.
- Feng, J.; Liu, T.; Du, Y.; Guo, S.; Lin, Y.; and Li, Y. 2025. CityGPT: Empowering Urban Spatial Cognition of Large Language Models. In *Proceedings of the 31th ACM SIGKDD International Conference on Knowledge Discovery and Data Mining*.
- Gurnee, W.; and Tegmark, M. 2024. Language Models Represent Space and Time. arXiv:2310.02207.
- Gururangan, S.; Marasović, A.; Swayamdipta, S.; Lo, K.; Beltagy, I.; Downey, D.; and Smith, N. A. 2020. Don't Stop Pretraining: Adapt Language Models to Domains and Tasks. In Jurafsky, D.; Chai, J.; Schluter, N.; and Tetreault, J., eds., *Proceedings of the 58th Annual Meeting of the Association for Computational Linguistics*, 8342–8360. Online: Association for Computational Linguistics.
- Haklay, M.; and Weber, P. 2008. OpenStreetMap: User-Generated Street Maps. *IEEE Pervasive Computing*, 7(4): 12–18.
- Herfort, B.; de Albuquerque, J. P.; Anderson, J.; and Zipf, A. 2021. OpenStreetMap Data Use Cases During the Early Months of the COVID-19 Pandemic. *ISPRS International Journal of Geo-Information*, 10(6): 402.
- Huang, J.; Wang, H.; Sun, Y.; Shi, Y.; Huang, Z.; Zhuo, A.; and Feng, S. 2022. ERNIE-GeoL: A Geography-and-Language Pre-trained Model and its Applications in Baidu Maps. In *Proceedings of the 28th ACM SIGKDD Conference on Knowledge Discovery and Data Mining, KDD '22*, 3029–3039. New York, NY, USA: Association for Computing Machinery. ISBN 9781450393850.
- Humanitarian OpenStreetMap Team. 2023. Using OSM Data for the Turkey and Syria Earthquake Response. <https://www.hotosm.org/updates/using-osm-data-for-the-turkey-and-syria-earthquake-response/>.
- Imran, M.; Castillo, C.; Lucas, J.; Meier, P.; and Vieweg, S. 2014. AIDR: artificial intelligence for disaster response. In *Proceedings of the 23rd International Conference on World Wide Web, WWW '14 Companion*, 159–162. New York, NY, USA: Association for Computing Machinery. ISBN 9781450327459.
- Ji, Y.; Gao, S.; Nie, Y.; Majić, I.; and Janowicz, K. 2025a. Foundation models for geospatial reasoning: assessing the capabilities of large language models in understanding geometries and topological spatial relations. *International Journal of Geographical Information Science*, 1–38.
- Ji, Y.; Gao, S.; Nie, Y.; Majić, I.; and Janowicz, K. 2025b. Foundation models for geospatial reasoning: assessing the capabilities of large language models in understanding geometries and topological spatial relations. *International Journal of Geographical Information Science*, 0(0): 1–38.
- Jiang, Y.; Chao, Q.; Chen, Y.; Li, X.; Liu, S.; and Cong, G. 2024. UrbanLLM: Autonomous Urban Activity Planning and Management with Large Language Models. In *Findings of the Association for Computational Linguistics: EMNLP 2024*, 1810–1825.
- Klaptocz, A. 2015. Mapping Nepal After the Earthquake. *WIRED*.
- Kojima, T.; Gu, S. S.; Reid, M.; Matsuo, Y.; and Iwasawa, Y. 2022. Large Language Models are Zero-Shot Reasoners. In *Advances in Neural Information Processing Systems*, volume 35, 22199–22213.
- Kolivand, P.; Saberian, P.; Tanhapour, M.; Karimi, F.; Rostam Niakan Kalhori, S.; Javanmard, Z.; Heydari, S.; Talari, S. S. H.; Laal Mousavi, S. M.; Alidadi, M.; Ahmadi, M.; and

Ayyoubzadeh, S. M. 2024. A systematic review of Earthquake Early Warning (EEW) systems based on Artificial Intelligence. *Earth Science Informatics*, 17(2): 957–984.

Li, Z.; Kim, J.; Chiang, Y.-Y.; and Chen, M. 2022. SpaBERT: A Pretrained Language Model from Geographic Data for Geo-Entity Representation. arXiv:2210.12213.

Li, Z.; Zhou, W.; Chiang, Y.-Y.; and Chen, M. 2023. GeoLM: Empowering Language Models for Geospatially Grounded Language Understanding. arXiv:2310.14478.

Manvi, R.; Khanna, S.; Mai, G.; Burke, M.; Lobell, D. B.; and Ermon, S. 2024. GeoLLM: Extracting Geospatial Knowledge from Large Language Models. In *The Twelfth International Conference on Learning Representations*.

Nearing, G.; Cohen, D.; Dube, V.; Gauch, M.; Gilon, O.; Harrigan, S.; Hassidim, A.; Klotz, D.; Kratzert, F.; Metzger, A.; Nevo, S.; Pappenberger, F.; Prudhomme, C.; Shalev, G.; Shenzis, S.; Tekalign, T. Y.; Weitzner, D.; and Matias, Y. 2024. Global prediction of extreme floods in ungauged watersheds. *Nature*, 627(8004): 559–563.

Pereira, J.; Lotufo, R.; and Nogueira, R. 2023. Large Language Models in Summarizing Social Media for Emergency Management. In Soboroff, I.; and Ellis, A., eds., *Proceedings of the 32nd Text Retrieval Conference*.

Rector, D. 2022. Power Outages, Communication Failures & Healthcare. <https://www.domesticpreparedness.com/articles/power-outages-communication-failures-healthcare>.

Roberts, J.; Lüddecke, T.; Das, S.; Han, K.; and Albanie, S. 2023. GPT4GEO: How a Language Model Sees the World's Geography. arXiv:2306.00020.

Singh, H.; Ang, L.; and Srivastava, S. K. 2025. Active wildfire detection via satellite imagery and machine learning: an empirical investigation of Australian wildfires. *Natural Hazards*, 121(8): 9777–9800.

UNDRR. 2020. The Human Cost of Disasters: An Overview of the Last 20 Years, 2000–2019. Technical report, UNDRR.

University of Central Florida. 2025. The Disaster Management Cycle. <https://www.ucf.edu/online/leadership-management/news/the-disaster-management-cycle/>.

Unlu, E. 2023. Chatmap : Large Language Model Interaction with Cartographic Data. arXiv:2310.01429.

Wei, J.; Tay, Y.; Bommasani, R.; Raffel, C.; Zoph, B.; Borgeaud, S.; Yogatama, D.; Bosma, M.; Zhou, D.; Metzler, D.; Chi, E. H.; Hashimoto, T.; Vinyals, O.; Liang, P.; Dean, J.; and Fedus, W. 2022. Emergent Abilities of Large Language Models. arXiv:2206.07682.

WFP, Google research. 2024. SKAI: Unleashing the Power of Artificial Intelligence to Revolutionize Disaster Response and Humanitarian Aid. <https://innovation.wfp.org/project/SKAI>.

Zhang, Y.; Wei, C.; He, Z.; and Yu, W. 2024. GeoGPT: An assistant for understanding and processing geospatial tasks. *International Journal of Applied Earth Observation and Geoinformation*, 131: 103976.